EUROfusion

WPDTT1-PR(17) 18605

G Mazzitelli et al.

First tokamak experiments with a liquid tin limiter

Preprint of Paper to be submitted for publication in
Physical Review Letters

This work has been carried out within the framework of the EUROfusion Consortium and has received funding from the Euratom research and training programme 2014-2018 under grant agreement No 633053. The views and opinions expressed herein do not necessarily reflect those of the European Commission.

First tokamak experiments with a liquid tin limiter

Mazzitelli G.[*], Apicella M.L., Iafrati M., Apruzzese G., Crescenzi F., Gabellieri L., Mancini A., Marinucci M., Romano A. and the FTU Team[*]

ENEA-Frascati, Via E. Fermi 45, 00044 Frascati Italy

Abstract

For the first time in a tokamak device, a Capillary Porous Liquid Tin Limiter (TLL) was exposed as plasma facing components in the FTU (Frascati Tokamak Upgrade). The TLL was progressively inserted deeply in the scrape-off-layer (SOL) very close to the last closed magnetic surface (<0.5cm). Spectroscopic measurements, a fast IR camera and Langmuir probes monitored the evolution of tin emission, tin surface temperature and heat loads on the limiter. The surface temperature rose up to 1700 °C in the hottest limiter region, a value for which tin evaporation is very high. Heat loads in excess of 15 MW/m^2 for 1 s were withstood by the TLL as deduced from Langmuir probes. Numerical simulations performed with the ANSYS code are in agreement with the experimental data taking into account the heat loads deposition profile on the TLL. As long as the surface temperature of the tin limiter is below 1300 °C, the main tin production mechanism is sputtering and the presence of such impurity in the discharge is negligible. When evaporation becomes dominant beyond 1300 °C tin is the main impurity present in the plasma. Nevertheless, the concentration of tin is in the order of 5x10^{-4} of the electronic density and no degradation in plasma performance has been observed. These results confirm the potentially major advantage of liquid tin as a PFC solution to the power exhaust for a fusion power plant.

Introduction

The problem of power exhaust is one of the major issues to solve for a future fusion reactor [1]. The erosion lifetime and power handling capability of the divertor plates must be compatible with the power and particle fluxes on them. Tungsten is currently the main candidate for the divertor plates as plasma facing component (PFC). But, to avoid a very short lifetime of the divertor plates, it must simultaneously fulfil two stringent conditions: an average power of less than 10 MW/m^2 with slow transients below 20 MW/m^2 and an electron temperature [2] below 5 eV. In the only possible plasma scenario more than 90% of the power will be radiated in the centre and/or SOL and the plasma will be partially detached.
As a risk mitigation strategy, two alternative solutions have been proposed. The first mainly implies modifications of the edge magnetic configuration in order to increase the wetted area by the plasma (snowflakes, super X divertor, double null configurations, etc.) [3]. The second one is the use of liquid metals as plasma facing components that for their potential capability to sustain s high heat flux, and, especially for tin, to meet the high core radiation requirement. Furthermore, solid materials are subject to erosion with dust formation and deterioration of their thermo-mechanical properties due to intense hydrogen and helium influx and

neutron irradiation while the use of liquid metals can improve the lifetime and reliability of PFCs.
In the last decade many experiments have been performed on different devices [4-9], which employed liquid metal limiters and divertors. In all these experiments lithium was chosen as liquid metal. Lithium is a low Z material (Z=3), which allows for better plasma performance, but its operational window is very narrow to avoid strong evaporation. Li liquefies at 180°C and evaporation becomes very large when the temperature of the liquid exceeds 550 °C. Nevertheless a vapor-box divertor has been proposed as possible solution for a future reactor [10].
Among the other possible liquid metals, tin has been identified as the best candidate having a large operation window, 300< T <1300 °C, low or negligible activation and low H retention [11]. Corrosion limits tin compatibility with many materials but in the temperature range of interest, it is possible to use Mo and W [12].
Tin is a high Z element, i.e. Z=50, lower than W but nevertheless it is crucial to demonstrate that plasma operations are possible at a tolerable Z_{eff} value without plasma performance degradation. This means that to keep Z_{eff} ~2 [2], the maximum tolerable tin concentration for DEMO should be less than 10^{-3} of the electron density [13]
In this letter we report experimental results obtained, for the first time in the world, in a tokamak with a liquid tin limiter. We have exposed the limiter to the plasma and increased the heat loads on the limiter from shot to shot to study the effects on the limiter itself and on the plasma performances. In particular we have looked at possible limiter damages and at the tin influx into the plasma core by monitoring its line emissions with a VUV survey instrument. On FTU the heat load on the limiter was high enough to reach a surface temperature, for more than 500ms, for which evaporation took place and tin was the main impurity present in the plasma.

Experimental set-up

In fig. 1 the TLL is shown. On the top a molybdenum tube is visible, on which Capillary Porous System (CPS) stripes made by tungsten felt filled with tin are wrapped [14]. The bending radius (r_{TLL}=129 cm) of the TLL in the poloidal direction is much greater than the minor radius of the plasma (a=29 cm) so that plasma does not homogenously wet the TLL. The high TLL bending radius was a technological compromise during the fabrication of the TLL head for a better and easier alignment of the CPS stripes. The TLL can be cooled by flowing air and atomized water in a copper tube inserted in the molybdenum pipe. In this letter we report only on experimental results that were obtained without an active cooling system.
The liquid metal limiter is inserted from a vertical port at the bottom side of the machine and its radial position can be varied shot by shot from the radius of the vacuum chamber wall (r=33.5 cm) up to r = 28.0 cm, which is 1.0 cm closer to the plasma centre than the TZM toroidal limiter (r=29.0 cm). After plasma exposure it can be extracted in a separate volume where an optical window permits a visual inspection of the TLL surface (see fig. 2).
The TLL limiter is equipped with several thermocouples and four Langmuir probes (see fig. 1), two for each side. The surface temperature of the TLL limiter is recorded with a fast infrared camera observing the whole TLL surface from the top of the FTU machine *(see fig 2)* (≅ 1 mm of spatial resolution and up to 1200 frames/s of acquisition rate). *A telescope placed on the same vertical port and connected by an*

optical fiber to an optical multichannel analyzer (OMA) monitors the production of tin from the limiter during the discharge. The amount of tin inside the plasma column is monitored by a VUV spectrometer SPRED [15] equipped with two interchangeable gratings respectively covering the range between 10-30nm and 20-160nm. The VUV survey instrument is mounted on an equatorial port and views the plasma along a central chord. It is located 90° away from the TLL in toroidal direction.

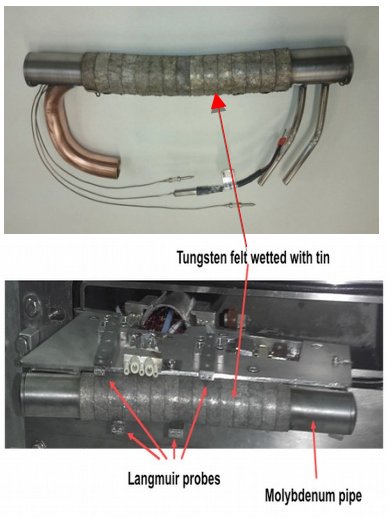

Fig 1: The Tin limiter

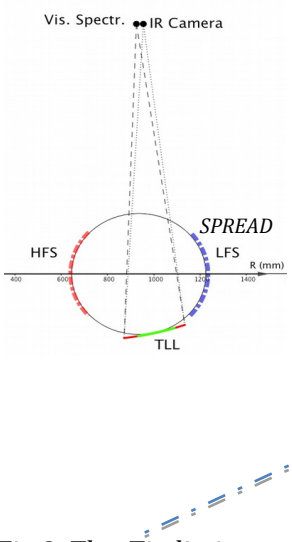

Fig 2. The Tin limiter set-up on FTU- In red on the high magnetic field side (HFS) the toroidal limiter and in blue in the low field magnetic side(LFS) the poloidal limiter . On top the IR Camera and the visible spectroscopy located on the vertical port outside the vacuum vessel. It is also shown the line of sight of the SPREAD located 90° away in toroidal direction.

Experimental results

In this first experimental campaign with the tin limiter a standard FTU discharge was used with a toroidal field B_t = 5.3 T, a plasma current I_p = 0.5 MA and a flat-top duration of 1.3 sec. The thermal load on the limiter was progressively varied either by moving up the limiter shot by shot in the scrape-off-layer (SOL), until almost reaching the last closed magnetic surface (LCMS), or by increasing the electron density at fixed limiter radial position as the electron temperature in the SOL of the FTU standard discharge of approximately 20 eV is almost independent of electron density [16].

We started our experiments with a series of standard discharges at fixed average electron density n_e=6x10^{19} m^{-3} moving the TLL in the SOL. In fig. 3 a,b the values for T_e and n_e as measured by the Langmuir Probes (LP) are given versus the distance from the LCMS. The e-folding lengths of temperature, density and heat load, as calculated by fitting the experimental data are respectively: $\lambda_{T,LP}$ =4.0±0.60 cm, $\lambda_{n,LP}$ =2.0 ±0.30 cm , $\lambda_{q,LP}$ =1.2 ±0.18 cm.

In fig. 3c the heat loads are shown as calculated using the well known formula [17]:

$$q_{LP} = \gamma J_{sat} T_e \quad (1)$$

where q_{LP} is the heat load onto the probes, γ=7.5 is the sheath energy transmission factor, J_{sat} is the ion saturation current density and $T_{e,}$ is the electron temperature. The presence of the TLL did not change the plasma characteristics of the FTU SOL in terms both of the absolute value of T_e and n_e as well as of the e-folding lengths [16]. The maximum heat load onto the Langmuir probes for these discharges was about q_{LP} = 5MW/m^2. Even though the Langmuir probes are not located in the most exposed region of the TLL, as it is possible to see in fig. 4 where the 2D image recorded by the infrared camera at time t = 1.5 s is shown, and do not have the same orientation, it is possible to deduce the heat load onto the entire limiter using the its geometry and the LCMS shape as reconstructed by the magnetic measurements. For these discharges the peak heat flux was about q_{max}= 10 MW/m^2.

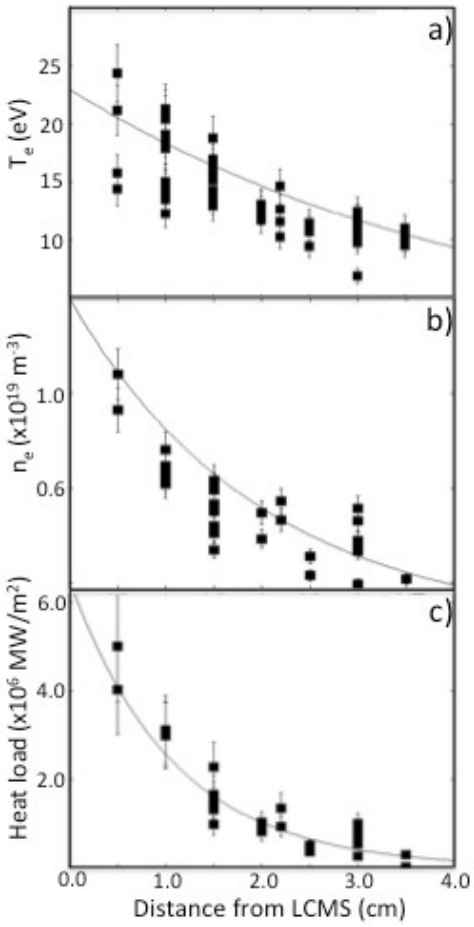

Fig 3 a) the electron temperature $T_{e,LP}$, b) the electron density $n_{e,LP}$, c) the heat load q_{LP} versus the distance from the LCMS. The lines are the exponential curve fits.

From Figure 4 it is clear that the plasma does not uniformly wet the surface of the limiter with asymmetries in both the toroidal and the poloidal direction. The shadows of the Langmuir probes (see fig. 1) are also clearly visible. The poloidal asymmetry is due to the different radius of the plasma curvature with respect to the tin limiter curvature radius (see fig. 2), while the toroidal asymmetry is due to the different connection lengths of the two sides of the toroidal limiter. In fig. 5, using a field line tracing code, the magnetic field line geometry has been reconstructed. The blue line does not touch the TLL limiter on the bottom of the figure, while the length of the red line is different for the two limiter sides. We have highlighted this difference in fig 5 by using a full red line for one side and a dotted red line for the other side. The length of the different red portions is about in the ratio 1:4, in a quite good agreement with the observed asymmetry in the surface temperature.

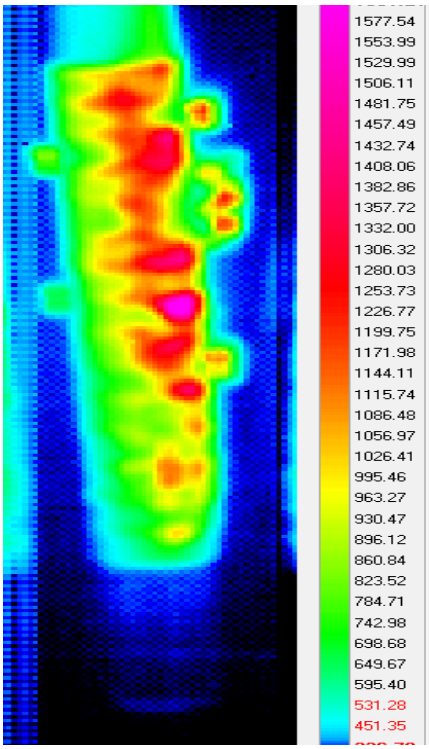

Fig. 4 2-D surface TLL temperature taken at the end of the current flat top.

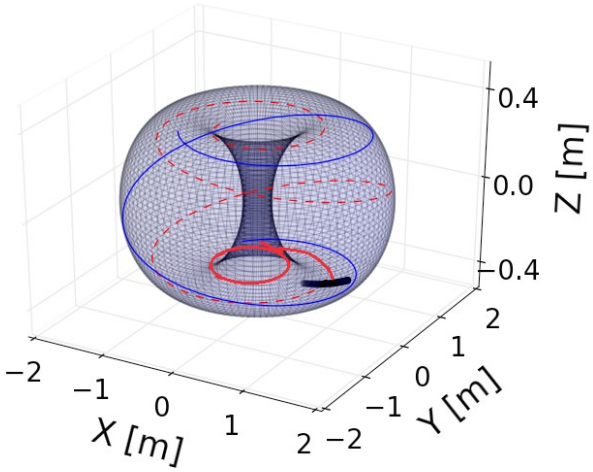

Fig 5. Magnetic field line pattern. On the bottom the black full line is the TLL limiter. The ray tracing show clearly that the two TLL sides, full and dotted red lines, are connected to the wall/limiters with different connection lengths. The blue line is a passing field line that does not intercept the TLL. The z-axis (vertical direction) is not in scale with the x-axis(radial direction) and y-axis(toroidal direction)

For these pulses the maximum surface temperature measured by the IR fast camera on the tin limiter was approximately $T_{s,max=}$ 1300 °C. (See fig. 9b)

In a second series of experiments we have increased the heat load on the TLL by changing the average electron density from 0.6 to 1.0x10^{20} m^{-3}. In fig. 6 the time evolution for the electron density and temperature as measured by the Langmuir probes is shown together with that of the heat load calculated using the formula (1) for two pulses in which the TLL was in the same position (0.5 cm from the LCMS). Even though the electron density for shot #41546 increases almost linearly and, at the end of the pulse, is about a factor 4 greater than in shot #41215, the electron temperature remains practically unchanged and consequently, the thermal load onto the TLL increases proportionally with the electron density reaching a value greater than q_{LP} = 15MW/m^2 for almost 1 s in pulse #41546.
If we compare pulse 41546 with pulse 41215, the main difference is on impurity production because in the former, as expected, pulse evaporation becomes the dominant tin production mechanism when the maximum surface temperature ($T_{s,max}$) of the limiter exceeds 1300 °C [18].

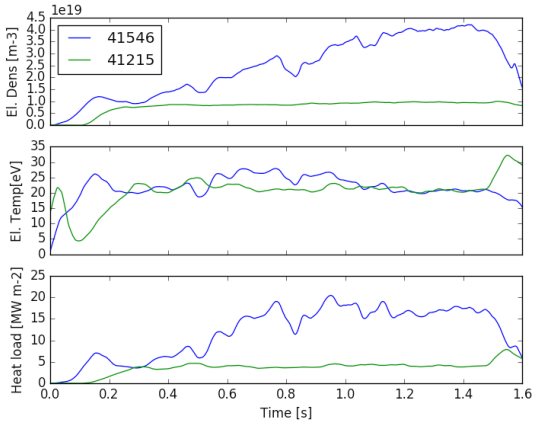

Fig. 6 from the top, the electron density $n_{e,LP,}$ the electron temperature $T_{e,LP}$ and the heat loads q_{LP} versus time are shown for two pulses.

The surface temperature of the hottest region of the limiter for pulse 41546 is plotted versus time in fig. 7, together with the plasma current $I_{p,}$ and the measured Sn XXI line emission. The Sn line emission starts to increase at 0.8 s at a surface temperature of $T_{s,max}$≈1300°C. Then we have had a problem with the magnetic vertical field also visible on the plasma current and there is a decrease in the surface temperature before starting to grow again. For t > 1 sec, when $T_{s,max}$ is well above 1300°C and the TLL hot surface is wider, the tin line begins to grow almost exponentially.

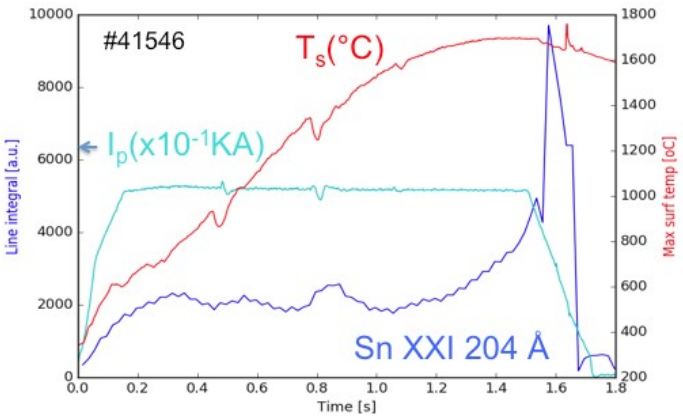

Fig. 7 Plasma current (cyan line), the surface temperature (red line) and the Sn XXI 204 Å line emission (blue line) are plotted versus time. The three overshoots in the plasma current and surface temperature traces were due to problems on the power supply of the vertical field control coils.

The presence of tin, when evaporation becomes the main impurity production mechanism, is even more evident on the UV spectrum. In fig. 8 we compare the VUV spectra for shot 41215 and shot 41547 (alike shot 41546 in which a different grating was used on SPRED).

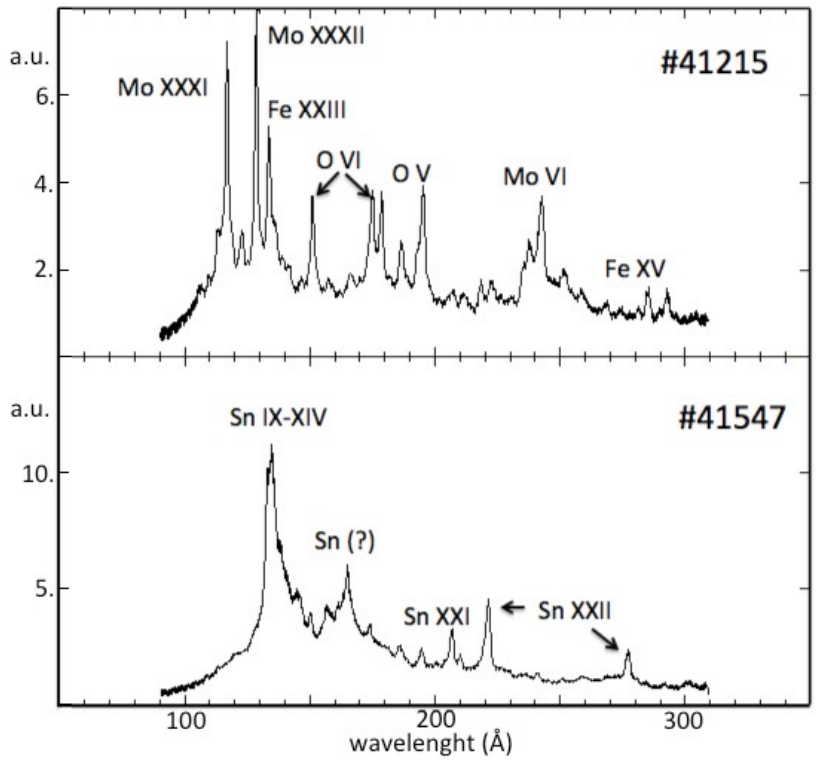

Fig. 8 On the top VUV spectra for shot #41215 and on the bottom for shot 41547 taken at the same time t= 1.2 s but different average electron densities n_e=0.6x10^{20} m^{-3} and n_e=1.0x10^{20} m^{-3}, respectively.

The lines of Mo and O dominate the spectrum of pulse 41215 and no lines of tin are detected, while the lines of tin exclusively dominate the spectrum of pulse 41547. In this spectrum are clearly visible the intense band emission between 130-140 Å due to emission of different ions Sn IX- Sn XII and the intense Zn-like and Cu like lines respectively at Sn XXI 204 Å (I.P. = 608 eV) and Sn XXII 276 Å (I.P. = 645 eV) that were also observed in tin injection on MAST [19]. The electron temperature at the centre of the plasma ranged from 1.0 to 1.4 KeV that it means that taking into account their ionization potential (I.P.) these ions should exist around half radius, i.e. well inside the last closed magnetic surface. The TLL interacting surface is about 10^{-2}-10^{-3} times the toroidal limiter surface wetted by the plasma that can explain the lack of tin lines, when sputtering and not evaporation is the dominant tin production mechanism as also confirmed by visible spectroscopy. A very small signal of Sn II emission was detected by the spectrometer looking directly to the tin limiter on shot #41215. On the contrary when evaporation becomes dominant this signal is much higher. As in the case of Li [20], for shot #41215 the Sn visible line emission is proportional to the D_α line emission pointing out that sputtering is the dominant mechanism of tin production. On the contrary, when the tin visible line and D_α line emission are not correlated the evaporation process dominates. Furthermore prompt redeposition of Tin on the limiter itself could contribute to reduce the tin influx in the discharge [21].

This dominance of the VUV spectrum by the liquid metal lines when evaporation is strong has already been observed on FTU with Li [22]. The reason why the other lines in the VUV spectra disappear is still being investigated. A possible explanation is that the plasma itself deposits on the TZM tiles of the toroidal limiter a thin layer

of evaporated liquid metal so that the sputtering of Mo atoms is strongly reduced. After a pulse with strong tin evaporation, one or two pulses without the liquid metal limiter are sufficient to clean the TZM tiles, so that the tin line emissions are no more detectable and the VUV spectrum is similar to ones on the top of fig 8.
Finally a 3D finite-element code ANSYS [23] has been used to reproduce the TLL surface temperature and to calculate the maximum heat load withstood by the limiter. A 3D real design of the limiter was used for the simulations and for CPS the ratio of the volume fraction between W and Sn was 66:34 as determined in laboratory tests. The limiter dimensions are smaller than those of the port through which it is inserted into the vacuum chamber and is therefore not in thermal contact with it. In these experiments the limiter was not actively cooled and the cooling channel filled with air, which is taken into account in the ANSYS runs. We have modelled the heat load on the TLL taking into account the distance of the limiter from the LCMS and the shape of the LCMS as reconstructed from the magnetic measurements. In fig. 9 a) and b) the comparison between ANSYS and the experimental results of the IR data is shown for the same shots of fig. 6. The plotted surface temperatures are relative to the hottest region of the tin limiter.

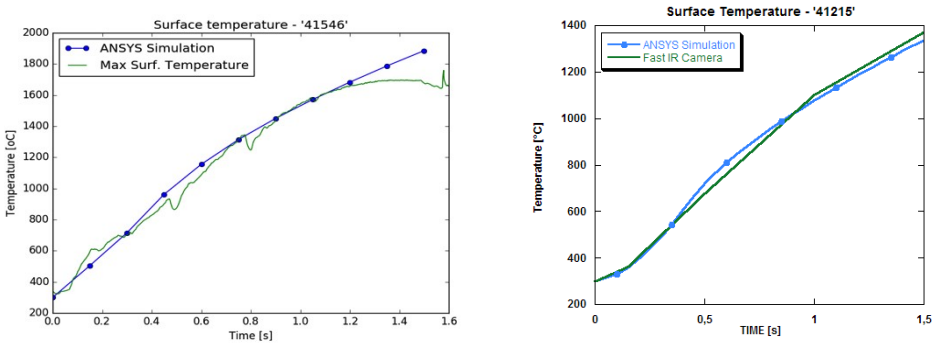

Fig 9 a,b The evolution of the TLL surface temperatures for the hottest region and the corresponding ANSYS simulation are shown for the pulses 41546 (q^{max}=18 MW/m^2) and 41215 (q^{max}=11 MW/m^2).

The surface temperature evolutions were modelled assuming an increasing heat load from the beginning of the pulse up to 0.4 s and then a constant heat flux of q^{max} =18 and 11 MW/m^2, respectively.
The reason for the difference between the heat load values used in the ANSYS simulations and those shown in fig. 6 is twofold: first, the maximum heat load on TLL does not coincide with the Langmuir probe positions. Second the position of the FTU magnetic axis as deduced from the magnetic measurements is not the same for the two pulses but there is a shift of about 1 cm. This shift has been also observed on the IR camera signals. This means that in the two analyzed shots the distance of the Langmuir probes from the maximum heat lead is different as confirmed by the IR camera.
The agreement in fig.9a and b is good, which confirms the consistency of the experimental data. It was sufficient to give as input to ANSYS the experimental data to reproduce the surface temperature time evolution without any further assumptions for matching two different shots. The good agreement between experimental data and ANSYS simulation remains also if we consider different

regions on the TLL surface.
It is important to note that in fig. 9a the deviation of the measured surface temperature from the simulated surface maximum temperature for t > 1.2 s could be due to the development of a tin cloud (vapor shield) near the TLL limiter as observed on Pilot PSI experiments [21], but more data are necessary to assess this effect.
No droplets have been observed entering into plasma during all the FTU experimental campaign and no damages were observed on the TLL after the plasma exposition. The CPS surface remains wetted by the tin and there is no apparent damage to the W CPS strips and no droplet production was observed, in agreement with expectations from stability analysis against Kelvin-Helmholtz and Rayleigh-Taylor instabilities [24].
Finally the effects on plasma performance were evaluated specially when tin evaporation was dominant. If we assume (see fig. 8b) that the only impurity present in the plasma column is tin we can deduce from the measured Z_{eff} value a concentration of tin of about 5 10^{-4} of the electron density. The JETTO code [25] was used to compare two similar discharges without and with the tin limiter in which tin evaporation was strong. The confinement time was within the error bars (10-15%) practically the same without any degradation in plasma performance.

In summary, for the first time in the world, a CPS tin limiter has been exposed to a tokamak plasma. The limiter was not actively cooled and plasma duration was limited; nevertheless these experiments demonstrated that liquid materials could support high heat loads in the same range as solid materials and with low plasma pollution. The good agreement between the measured and simulated surface temperature confirms what has been achieved on Pilot-PSI [21] with tin and the RACLETTE code calculations [18]: with an appropriate cooling system CPS divertor plates can withstand heat loads up to 20 MW/m^2 without tin evaporation. This letter is a fundamental step to solve the plasma exhaust problem and a first experimental demonstration that tin liquid metal can be a viable alternative solution to solve the power exhaust problem for DEMO.

The authors wish to thank Paolo Buratti and Holger Reimerdes for providing valuable input to the manuscript. This work has been carried out within the framework of the EUROfusion Consortium and has received funding from the Euratom research and training programme 2014-2018 under grant agreement No 633053. The views and opinions expressed herein do not necessarily reflect those of the European Commission

*giuseppe.mazzitelli@enea.it

[1] F. Romanelli Fusion Electricity – A roadmap to the realization of fusion energy, EFDA, 2012.
[2] G. Federici, R. Kemp, D. Ward, C. Bachmann, T. Franke, S. Gonzalez, C. Lowry, M. Gadomska, J. Harman, B. Meszaros, C. Morlock, F. Romanelli, R. Wenninger Fusion Eng. Des. 89 (2014) 882
[3] A.Loarte, R. Neu *on Fusion Eng. Des. (2017) http://dx.doi.org/10.1016/ j.fusengdes.2017.06.024*
[4] G. Mazzitelli, M.L. Apicella, D. Frigione, G. Maddaluno, M. Marinucci, C. Mazzotta, V. Pericoli Ridolfini, M. Romanelli, G. Szepesi, O. Tudisco and FTU Team, Nucl. Fusion 51 (2011) 073006

[5] M.A. Jaworski, T. Abrams, J.P. Allain, M.G. Bell, R.E. Bell, A. Diallo, T.K. Gray, S.P. Gerhardt, R. Kaita, H.W. Kugel, B.P. LeBlanc, R. Maingi, A.G. McLean, J. Menard, R. Nygren, M. Ono, M. Podesta, A.L. Roquemore, S.A. Sabbagh, F. Scotti, C.H. Skinner, V.A. Soukhanovskii, D.P. Stotler and the NSTX Team Nucl. Fusion 53 (2013) 083032

[6] G.Z. Zuo, J.S. Hu, R. Maingi, J. Ren, Z. Sun, Q.X. Yang, Z.X. Chen, H. Xu, K. Tritz, L.E. Zakharov, C. Gentile, X.C. Meng, M. Huang, W. Xu, Y. Chen, L. Wang, N. Yan, S.T. Mao, Z.D. Yang, J.G. Li and EAST Team, Nucl. Fusion 57 (2017) 046017

[7] R. Kaita, M. Lucia, J.P. Allain, F. Bedoya, R. Bell, D. Boyle, A. Capece, M. Jaworski, B.E. Koel, R. Majeski, J. Roszell, J. Schmitt, F. Scotti, C.H. Skinner, V. Soukhanovskii, Fusion Engineering and Design, Volume 117, (2017), 135-139

[8] S.V. Mirnov, A.M. Belov, N.T. Djigailo, A.S. Dzhurik, S.I. Kravchuk, V.B. Lazarev, I.E. Lyublinski, A.V. Vertkov, M.Yu. Zharkov and A.N. Shcherbak, Nucl. Fusion 55 (2015) 123015.

[9] J.Sánchez, M. Acedo, A. Alonso, J. Alonso, P. Alvarez, E. Ascasíbar, A. Baciero, R. Balbín, L. Barrera, E. Blanco, J. Botija, A. de Bustos, E. de la Cal, I. Calvo, A. Cappa, J.M. Carmona, D. Carralero, R. Carrasco, B.A. Carreras, F. Castejón, R. Castro, G. Catalán, A.A. Chmyga, M. Chamorro, L. Eliseev, L. Esteban, T. Estrada, A. Fernández, R. Fernández-Gavilán, J.A. Ferreira, J.M. Fontdecaba, C. Fuentes, L. García, I. García-Cortés, R. García-Gómez, J.M. García-Regaña, J. Guasp, L. Guimarais, T. Happel, J. Hernanz, J. Herranz, C. Hidalgo, J.A. Jiménez, A. Jiménez-Denche, R. Jiménez-Gómez, D. Jiménez-Rey, I. Kirpitchev, A.D. Komarov[2], A.S. Kozachok, L. Krupnik, F. Lapayese, M. Liniers, D. López-Bruna, A. López-Fraguas, J. López-Rázola, A. López-Sánchez, S. Lysenko, G. Marcon, F. Martín, V. Maurin, K.J. McCarthy, F. Medina, M. Medrano, A.V. Melnikov, P. Méndez, B. van Milligen, E. Mirones, I.S. Nedzelskiy, M. Ochando, J. Olivares, J.L. de Pablos, L. Pacios, I. Pastor, M.A. Pedrosa, A. de la Peña, A. Pereira, G. Pérez, D. Pérez-Risco, A. Petrov, S. Petrov, A. Portas, D. Pretty, D. Rapisarda, G. Rattá, J.M. Reynolds, E. Rincón, L. Ríos, C. Rodríguez, J.A. Romero, A. Ros, A. Salas, M. Sánchez, E. Sánchez, E. Sánchez-Sarabia, K. Sarksian, J.A. Sebastián, C. Silva, S. Schchepetov, N. Skvortsova, E.R. Solano, A. Soleto, F. Tabarés, D. Tafalla, A. Tarancón, Yu. Taschev, J. Tera, A. Tolkachev, V. Tribaldos, V.I. Vargas, J. Vega, G. Velasco, J.L. Velasco, M. Weber, G. Wolfers and B. Zurro, Nucl. Fusion 49 (2009) 104018

[10] R.J. Goldston , R. Myers, J. Schwartz, Phys. Scripta T167, 014017 (2016)

[11] J.P.S. Loureiro, F.L. Tabarés, H. Fernandes, C. Silva, R. Gomes, E. Alves, R. Mateus,T. Pereira, H. Alves, H. Figueiredo Fusion_Engineering_and Design_117_(2017)_208–211.

[12] A. Vertkov, I. Lyublinski, M. Zharkov, G. Mazzitelli, M.L. Apicella, M. Iafrati, Fusion Engineering and Design, 117, (2017), 130-134,

[13] *M.* Poradziński, I. Ivanova-Stanik, G. Pełka, R. Zagórski, http://dx.doi.org/10.1016/j.fusengdes.2017.04.131

[14] L.G. Golubchikov, V.A. Evtikhin, I.E. Lyublinski, V.I. Pistunovich, I.N. Potapov, A.N. Chumanov J. Nucl. Mater. 233–237 (1996) 667–72.

[15] R. J. Fonck, A. T. Ramsey, and R. V. Yelle. App. Optics, 21(12):2115, 1982.

[16] V. Pericoli Ridolfini, R. Zagórski, F. Crisanti, G. Granucci, G. Mazzitelli, L. Pieroni, F.Romanelli Journ. Nucl. Materials, **V. 220-222**, p. 218-222, (1995)

[17] P. C. Stangeby, The Plasma Boundary of Magnetic Fusion Devices (Taylor & Francis, London, 2000).

[18] J.W. Coenen, G. De Temmerman, G. Federici, V. Philipps, G. Sergienko, G. Strohmayer, A. Terra, B. Unterberg, T. Wegener, and D. C. M. Van den Bekerom, Phys. Scr. T159, 014037 (2014).

[19] A. *Foster, PhD Thesis,* University of Strathclyde, *2008*

[20] M. L. Apicella, G. Apruzzese, G. Mazzitelli, V. Pericoli Ridolfini, A. G. Alekseyev, V. B. Lazarev, S. V. Mirnov and R. Zagorski, Plasma Phys. Control. Fusion 54 (2012) 035001

[21] T.W. Morgan, D. C. M. van den Bekerom, and G.De Temmerman, J. Nucl. Mater. 463, 1256 (2015).

[22] G. Mazzitelli, M.L. Apicella, M.Marinucci, A. Alekseyev, G. Apruzzese, P. Buratti, R. Cesario, L. Gabellieri, V. Lazarev, I. Lyublinski, C. Mazzotta, S. Mirnov, V. Pericoli Ridolfini, A. Romano, O. Tudisco, A. Vertkov, R. Zagorski, FTU Team, ECRH Team, R. B. Gomes, H. Fernandes, C. Silva, C. Varandas, O. Lielausis, A. Klyukin and E. Platacis , Proc. 22th IAEA Fusion Energy Conf. 13-18 October 2008 Geneva, Switzerland, Paper EX /P4-6

[23] ANSYS Multiphysics 15.0 User Manual.

[24] G. Mazzitelli, M. L. Apicella, M. Iafrati, G. Apruzzese, A. Buscarino, G. Calabrò, C. Corradino, F. Crescenzi, L. Fortuna, G. Maddaluno, T. W. Morgan, G. Ramogida,and A. Vertkov,, Proc. 26th IAEA Fusion Energy Conf. 17-22 October 2016 Kyoto, Japan, Paper EX /P8-21

[25] G. Cenacchi and A. Taroni, in Proc. 8th Computational Physics, Computing in Plasma Physics, Eibsee 1986, (EPS 1986), Vol. 10D, 57.